

Accepted Manuscript

Improved catalytic activity of mixed platinum catalysts supported on various carbon nanomaterials

Jie Zhang , Shuihua Tang , Longyu Liao , Weifei Yu , Jinshan Li , Frode Seland , Geir Martin Haarberg



PII: S0378-7753(14)00830-1

DOI: [10.1016/j.jpowsour.2014.05.137](https://doi.org/10.1016/j.jpowsour.2014.05.137)

Reference: POWER 19220

To appear in: *Journal of Power Sources*

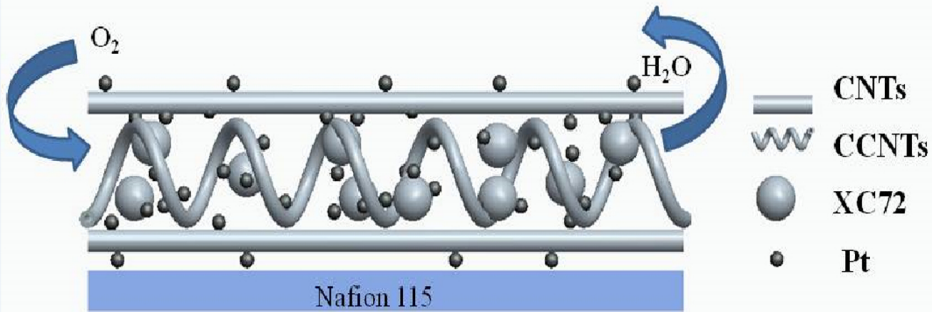
Received Date: 9 February 2014

Revised Date: 12 May 2014

Accepted Date: 27 May 2014

Please cite this article as: J. Zhang, S. Tang, L. Liao, W. Yu, J. Li, F. Seland, G.M. Haarberg, Improved catalytic activity of mixed platinum catalysts supported on various carbon nanomaterials, *Journal of Power Sources* (2014), doi: 10.1016/j.jpowsour.2014.05.137.

This is a PDF file of an unedited manuscript that has been accepted for publication. As a service to our customers we are providing this early version of the manuscript. The manuscript will undergo copyediting, typesetting, and review of the resulting proof before it is published in its final form. Please note that during the production process errors may be discovered which could affect the content, and all legal disclaimers that apply to the journal pertain.



1 Improved catalytic activity of mixed platinum 2 catalysts supported on various carbon nanomaterials

3 Jie Zhang ^{a,b,c}, Shuihua Tang ^{a,b,*}, Longyu Liao ^c, Weifei Yu ^{c,*}, Jinshan Li ^c,
4 Frode Seland ^d, Geir Martin HAARBERG ^d

5 ^aState Key Laboratory of Oil and Gas Reservoir Geology and Exploitation, Southwest
6 Petroleum University, Chengdu City, Sichuan 610500, PR China

7 ^bSchool of Materials and Engineering, Southwest Petroleum University, Chengdu City,
8 Sichuan 610500, PR China

9 ^cInstitute of Chemical Materials, China Academy of Engineering Physics, Mianyang
10 City, Sichuan 621900, PR China

11 ^dDepartment of Material Science and Engineering, Norwegian University of Science
12 and Technology, Trondheim 7491, Norway

13 *Corresponding author. Tel | Fax: +86 028 83032879.

14 E-mail address: shuihuatang@swpu.edu.cn (S.H. Tang).

15 Corresponding author. Tel | Fax: +86 0816 2480362.

16 E-mail address: yuwf_1988@sohu.com (W.F. Yu).

17

18 ABSTRACT

19 Electrocatalyst support affects not only catalytic activity of a catalyst, but also mass
20 transportation and electron transfer in the catalyst layers of an electrode for proton
21 exchange membrane fuel cells. Multi-dimensional and combined carbon materials
22 such as Vulcan XC-72, carbon nanotubes (CNTs), and home-made coiled carbon
23 nanotubes (CCNTs) are applied to enhance the catalyst activity and utilization. Three-
24 dimensional CCNTs with large specific surface area and graphitic characteristic are

synthesized by solid-state catalytic method. This obtained CCNTs and commercial CNTs are used as support to prepare platinum catalysts via modified ethylene glycol method, respectively. And the electrochemical surface areas (ECSAs) of the as-prepared Pt/CNTs, Pt/CCNTs and commercial Pt/C (JM) catalyst are evaluated by cyclic voltammetry. Then each two and three kinds of above catalysts mixed with different mass ratios are investigated. The ECSAs of Pt/C-Pt/CCNTs (95:5) and Pt/C-Pt/CNTs-Pt/CCNTs (80:10:10) are calculated to be $106 \text{ m}^2 \text{ g}_{\text{Pt}}^{-1}$ and $111 \text{ m}^2 \text{ g}_{\text{Pt}}^{-1}$, with respect to $70 \text{ m}^2 \text{ g}_{\text{Pt}}^{-1}$ of Pt/C (JM) catalyst. And these mixed catalysts also demonstrate improved oxygen reduction reaction activities. This is mainly attributed to the unique structure of CCNTs, which can construct a multi-dimensional network to facilitate the mass transportation and electrons/protons transfer.

Keywords:

Coiled carbon nanotubes

Carbon nanotubes

Oxygen reduction reaction

Catalytic activity

Proton exchange membrane fuel cells

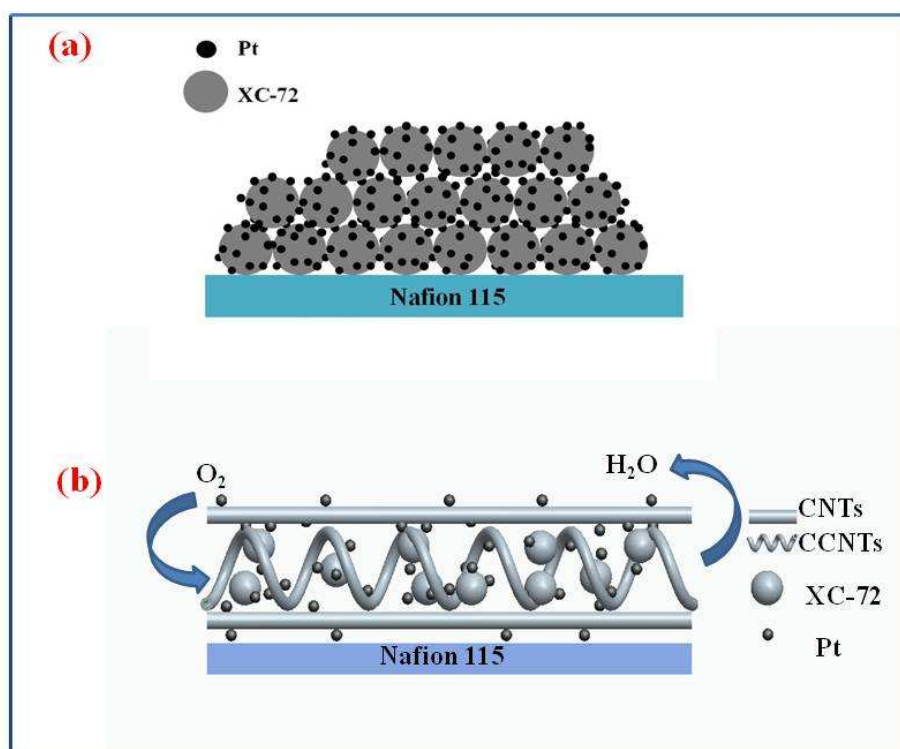
1. Introduction

Proton exchange membrane fuel cell (PEMFC) has been regarded as an attractive and efficient power supply for portable applications due to its high efficiency, high specific energy density, zero pollution, and low operation temperature [1-2]. Pt-based electrocatalysts, a kind of promising catalytic materials for widely-adopted PEMFC, provide remarkable activity for hydrogen oxidation and oxygen reduction reactions (ORR) [3]. While one important goal for commercialization of PEMFC is to reduce

the amount of platinum and enhance the cell performance [4]. It is generally accepted that performance is dependent on the shape, size, and distribution of Pt nanoparticles. In addition, supporting material could affect not only the catalytic properties but also mass transportation and electron transfer in catalyst layers of electrode, resulting in an enhanced catalytic activity [5]. Various carbon materials with different nanostructures and morphological characteristics have been used as support ranging from carbon black, carbon aerogels [6], carbon nanotubes, mesoporous carbon, and so on. Carbon blacks Vulcan XC-72 has been commonly used as support for electrocatalysts in PEMFC, but the utilization of XC-72 supported catalyst is usually less than 20% due to a close pack of catalyst particles during the hot-press process of membrane electrode assembly (MEA) fabrication [7]. Carbon nanotubes (CNTs), with the unique morphology and physical properties including a large aspect ratio, good electrical conductivity and mechanical stability, possess the ability to carry large current densities and offer channels for fast electron/proton transfer when used for PEMFC [8-10]. The carbon nanocoils (CNCs) also realize the requirement of an ideal support for electrocatalyst, mainly due to well-defined porosity, large specific surface area of $318 \text{ m}^2 \text{ g}^{-1}$, high degree of graphitization, and good crystallinity [11].

Recently the potential application of mixed electrocatalysts has been proposed to enhance the electrochemical property. Single-wall carbon nanotubes (SWNTs) and multi-wall carbon nanotubes (MWNTs) hybrids loaded with Pt, evaluating as the cathode catalyst layer in PEMFC, led to an increased mass transport characteristics and cathode-specific mass activity due to a combination of the increased mass activity caused by MWNTs and the efficient proton transfer ensured by SWNT network [12]. Shaijumon et al. [13] used [50% Pt/MWCNT + 50% Pt/C] as cathode electrocatalyst in PEMFC, and it showed the best performance of 288.9 mW cm^{-2} at voltage of 540

75 mV and current density of 535 mA cm^{-2} due to better dispersion of Pt nanoparticles
 76 and good accessibility of MWCNT. Graphene nanosheet (GN) also has opened up a
 77 new way for employing as support due to its unique morphology and super electronic
 78 conductivity [14-15]. Yang et al. [16] reported the Pd/GNS-CNTs (GN/CNTs=5:1)
 79 exhibited the highest electrochemical active surface area (ECSA) and Pd utilization,
 80 this indicated the excellent catalytic activity and stability for formic acid
 81 electrooxidation compared to Pd/Vulcan XC-72R, Pd/GNS, or Pd/CNTs catalysts.
 82 Jafri et al. [17] pointed out the mixture of functionalized multi-walled carbon
 83 nanotube (f-MWNT) and functionalized graphene (f-G) could also act as good
 84 catalysts supporting material for both methanol oxidation and ORR. The single cell
 85 with PtRu/ (50% f-G + 50 % f-MWNT) and Pt/ (50% f-G + 50% f-MWNT) gave a
 86 maximum power density of 68 mW cm^{-2} .



87
 88 **Fig. 1.** The schematic structures of (a) Pt/XC-72 and (b) Pt/XC-72-Pt/CNTs-Pt/CCNTs catalyst
 89 layer.

The structures of Pt/XC-72 and Pt/XC-72-Pt/CNTs-Pt/CCNTs catalyst layer are shown schematically in Fig. 1. Spherical XC-72 carbon black is a good catalyst support but its supported Pt catalysts are easily compressed during hot-press process, this will block reactants to get access to some active sites and reduce the catalyst utilization (as shown in Fig.1a); moreover, the electron conductivity of XC-72 is not very good. In this paper, three-dimensional coiled carbon nanotubes (CCNTs) with large specific surface area and graphitic characteristic will be applied to construct more effective mass transportation channels, and one-dimensional CNTs are expected to facilitate the electron transfer (as shown in Fig.1b). Then introduction of CCNTs and/or CNTs into the Pt/XC-72 catalysts will be designed to improve the catalytic activity and utilization of Pt/XC-72. Each two and three kinds of Pt/C, Pt/CNTs, and Pt/CCNTs catalysts will be mixed with different mass ratios and then investigated.

2. Experimental

2.1. Preparation of CCNTs

CCNTs was synthesized according to the method of heat-treating mixtures of carbon precursors, silica sol, and transition-metal salts [18]. Resorcinol-formaldehyde (RF) gel was chosen as carbon precursors. Iron nitrate was used as catalyst, and silica sol (AkzoNobel chemicals Corp., particle size of $\text{SiO}_2 = 4 \text{ nm}$; density = 1.1 g cm^{-3}) was added into the reaction mixture to achieve a high specific surface area and suitable pore size carbon material. The aqueous reaction mixture of iron nitrate/trisodium citrate/silica/resorcinol/formaldehyde with a molar ratio of 0.8:0.8:1:2:4, was cured at 85°C for 3 h, then carbonized in an argon atmosphere at 850°C for 3 h, followed by refluxing in 3 M NaOH to remove the silica particles and in 5 M HNO_3 to remove other residual. Eventually CCNTs was obtained after filtered, washed, and dried at 100°C in vacuum overnight.

2.2. Preparation of electrocatalysts

Pt catalyst supported on carbon material was prepared using an improved ethylene glycol method. The required amounts of chloroplatinic acid ($\text{H}_2\text{PtCl}_6 \cdot 6\text{H}_2\text{O}$) was added to ethylene glycol (EG) under magnetic stirring, and then the pH value of the solution was adjusted with sodium hydroxide. Subsequently, the required amounts of CNTs (Chengdu Organic Chemicals Company, China) or CCNTs was added into the resulting EG solution and the obtained reaction mixture was kept at 140 °C for 3 h with a reduction process. Finally, the resulting suspension was cooled, filtered, washed with deionized water until no chloride ions detected, and then dried in vacuum oven. The prepared catalysts are respectively denoted as 40 wt.% Pt/CNTs and 40 wt.% Pt/CCNTs. 40 wt.% Pt/C catalyst from Johnson Matthey Company (HiSPECTM 4000) was adopted as Pt/XC-72.

2.3. Physical characterization

The Brunauer-Emmett-Teller (BET) specific surface areas were measured by N_2 adsorption and Barrett-Joyner-Halenda (BJH) desorption method was applied to determine pore size distributions, using on a Quantachrome Nova Automated Gas Sorption System. The crystallinity of carbon materials and electrocatalysts was determined through X-ray diffraction (XRD) performed on a Rigaku D/MAX X-ray diffractometer equipped with Cu $\text{K}\alpha$ radiation operating on 40 kV. Raman spectra were measured at room temperature with the Raman system (JY-HR800). Morphologies of carbon material and catalysts were revealed by transmission electron microscopy (TEM, Carl Zeiss SMT, Libra 200FE).

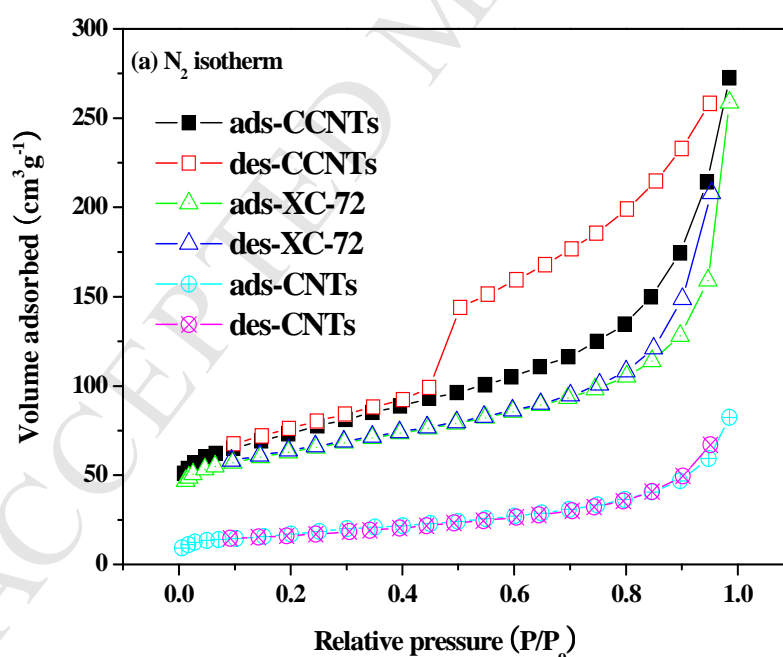
2.4. Electrochemical characterizations

Electrochemical measurements were performed using an AutoLab Potentiostat (Metrohm, Holland) with a three-electrode system at room temperature. 5 mg of the

electrocatalyst was ultrasonically suspended in 1 mL of ethanol and 50 μ L of Nafion[®] solution (5 wt%, Du Pont) for 30 min to form a homogeneous ink. Then 25 μ L of the ink was spread onto the surface of glassy carbon electrode (GC) with a diameter of 5 mm (geometric area of 0.196 cm²) embedded in a Teflon cylinder (Pine Instrument). A Pt wire and Ag/AgCl electrode were employed as the counter and the reference electrodes, respectively. Cyclic voltammetry (CV) was taken at room temperature between 0 and 1.4 V (vs. NHE) in 0.5 M H₂SO₄ with a scan rate of 20 mV s⁻¹. Linear sweep voltammetry (LSV) experiments were conducted in O₂-saturated 0.5 M H₂SO₄ at a scan rate of 10 mV s⁻¹ and rotation rate of 1600 rpm.

3. Results and discussion

3.1. Physical characterization of carbon materials and electrocatalysts



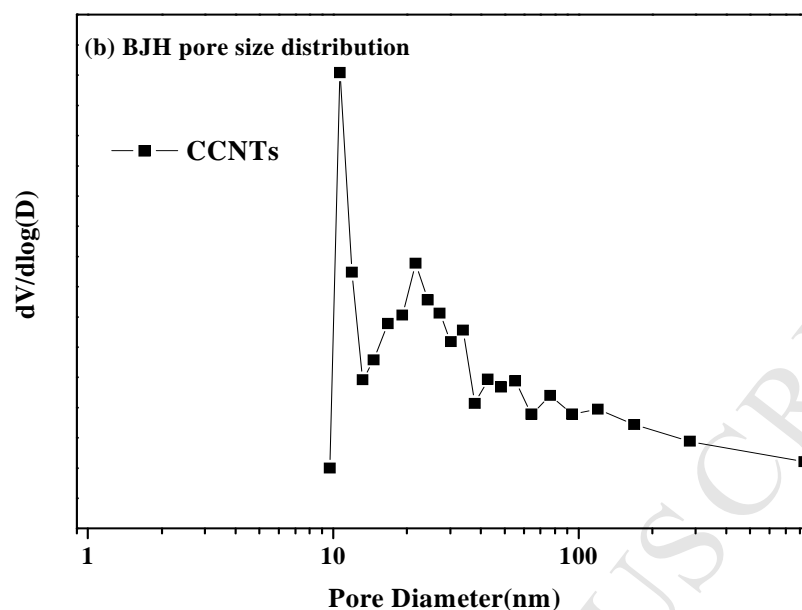


Fig. 2. (a) N_2 adsorption/desorption isotherm of carbon materials and (b) pore size distribution of CCNTs.

The specific surface areas of XC-72, CNTs, and CCNTs are measured to be 215, 61, and 404 $m^2 g^{-1}$. The increased adsorption branch at low relative pressure and the hysteresis loop for desorption branch under the higher relative pressures of CCNTs are observed in Fig. 2a, which attributes to the hysteresis loop of type-H1 [19]. Fig. 2b shows a pore distribution of CCNTs mainly ranging from 10 to 40 nm, which indicates a typical mesoporous structure. XC-72 possesses a significant amount of mesopores [20], but CCNTs exhibit much larger mesopore volume and specific surface area than those of XC-72 and CNTs.

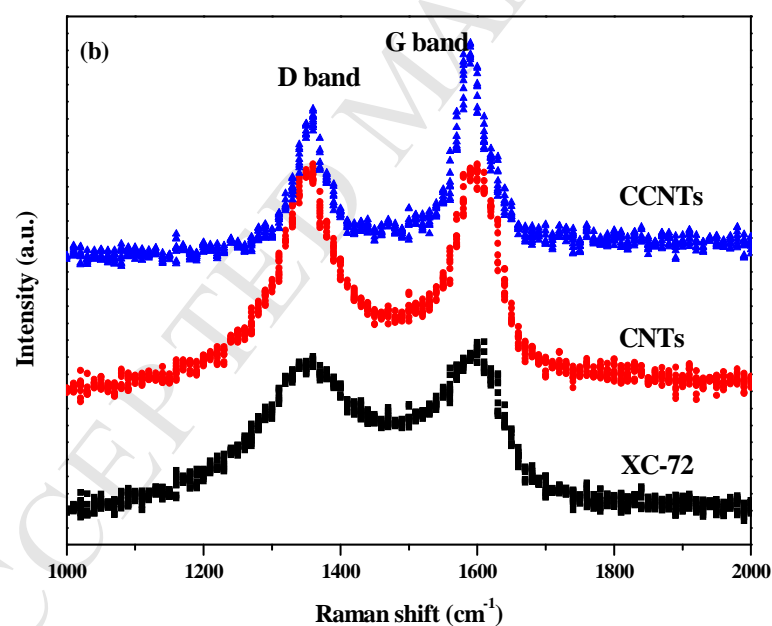
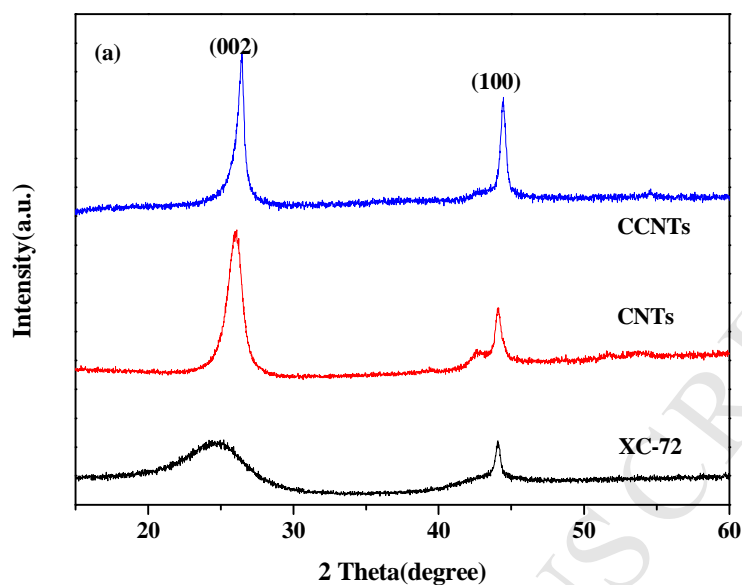


Fig. 3. (a) XRD patterns and (b) Raman spectra of various carbon materials.

Fig. 3a shows the XRD patterns of XC-72, CNTs, and CCNTs. It can be seen that CCNTs indicate intensive diffraction peaks corresponding to the (002) and (100) diffraction peaks of graphite. The (002) diffraction peak of CCNTs is sharper and more intense than that of the XC-72 or CNTs, indicating its excellent graphitic

properties. Compared to 0.3354 nm of graphite $d_{(002)}$ spacing [21], the $d_{(002)}$ of CCNTs is calculated to be 0.3387 nm using Bragg's equation based on the (002) diffraction peak, and its crystallinity is superior to that of CNTs (0.3438 nm) or amorphous XC-72 (0.3678 nm) [22]. According to Raman spectra, G ("graphite") band peak at 1590 cm^{-1} relates to the vibration of sp^2 -hybridized carbon, D ("defect") band peak at 1350 cm^{-1} corresponds to defects, and the intensity ratio between the D and G bands (I_D/I_G) is a measure of graphitic characteristic, and the lower I_D/I_G value means the higher graphitic property [23]. As shown in Fig. 3b, CCNTs possesses lower I_D/I_G value than XC-72 and CNTs, which means it has better graphitic characteristic. This further confirms the XRD result.

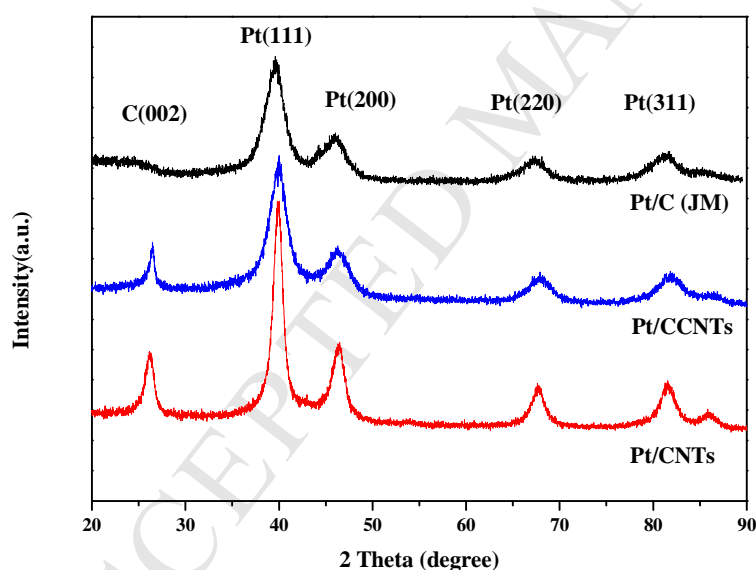
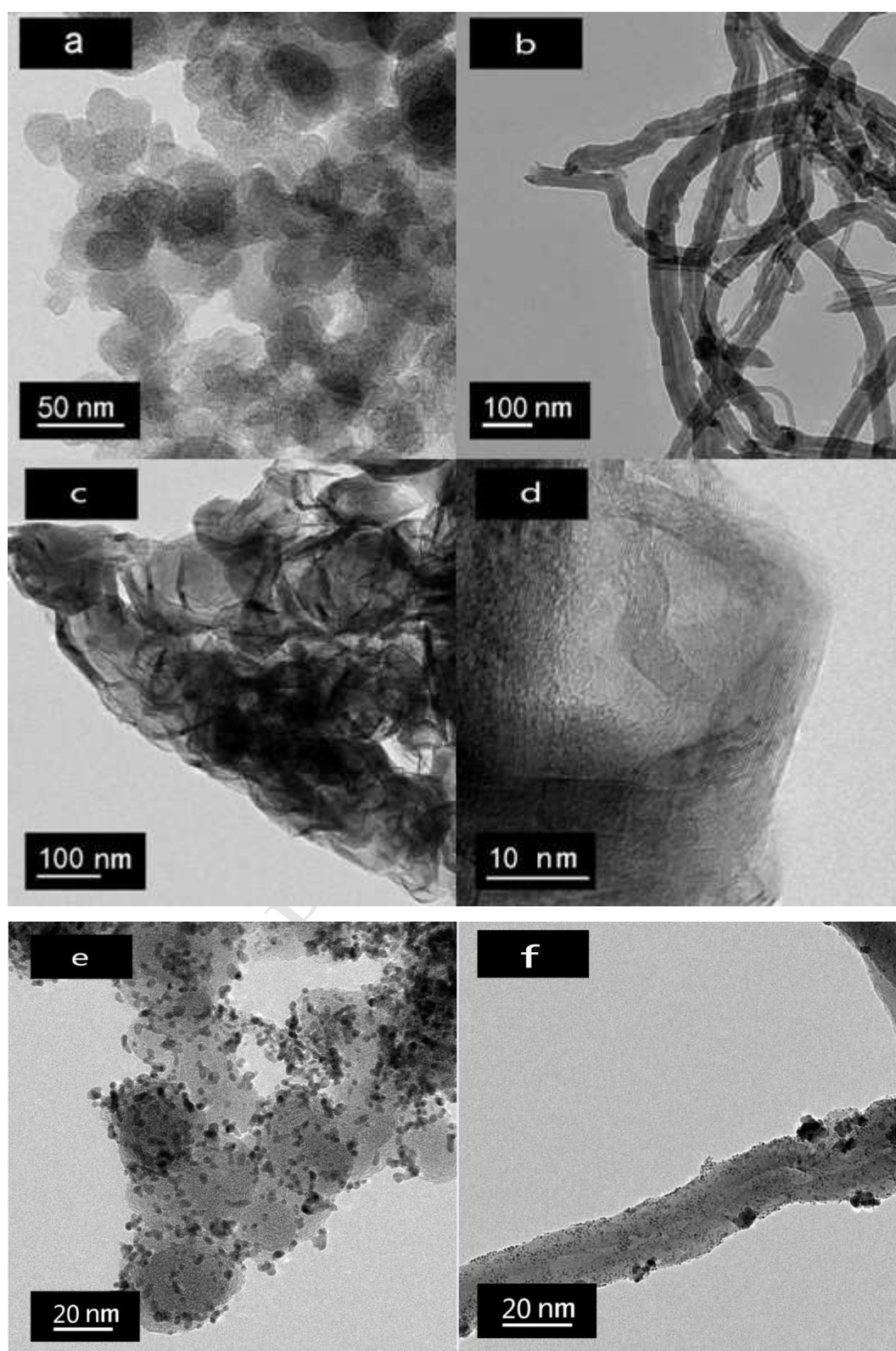


Fig. 4. XRD patterns of Pt catalysts supported on different carbon materials.

The XRD patterns in Fig. 4 show a f.c.c. Pt crystalline structure of Pt/CCNTs, Pt/CNTs, and Pt/C, which is inferred from Pt (111), (200), (220), and (311) four characteristic peaks located at 39.8° , 46.2° , 67.5° , and 81.2° . Pt (220) peak is isolated from the graphite diffraction peaks of carbon support [24], and the mean size of Pt

186 particles in Pt/CCNTs, Pt/CNTs, and Pt/C are calculated to be 3.7 nm, 5.8 nm, and 3.5
187 nm via Scherrer' formula.



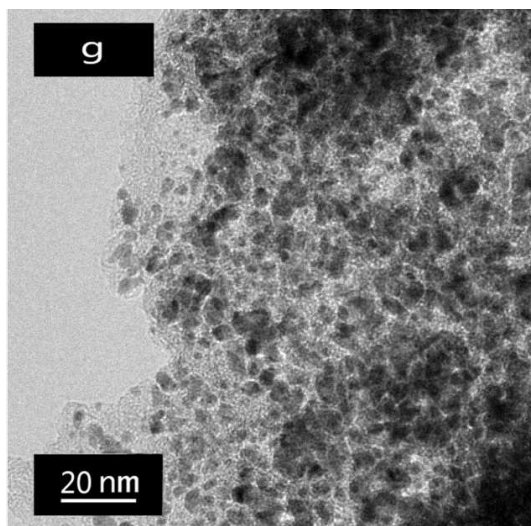


Fig. 5. TEM images of (a) XC-72, (b) CNTs, (c) and (d) CCNTs, (e) Pt/C (JM), (f) Pt/CNTs, and (g) Pt/CCNTs.

As a comparison, the TEM images of XC-72 and CNTs are shown in Fig. 5a and Fig. 5b. XC-72 consists of spherical carbon particles with diameters of 20 to 50 nm. Fig. 5c displays crystalline structure of CCNTs particles consisting of the graphitic coils with a wall thickness of 5 to 10 nm. The observed graphitic layers are consistent with the above XRD results. Fig. 5e and Fig. 5f clearly reveal Pt particles distributed uniformly with a size ranging from 3 to 4 nm on XC-72 and a size distribution of 5 to 7 nm on CNTs. As shown in Fig. 5g, Pt particles with size ranging from 3 to 5 nm are homogeneously dispersed on CCNTs. These agree well with the calculated results from XRD.

3.2. Electrochemical measurement of electrocatalysts

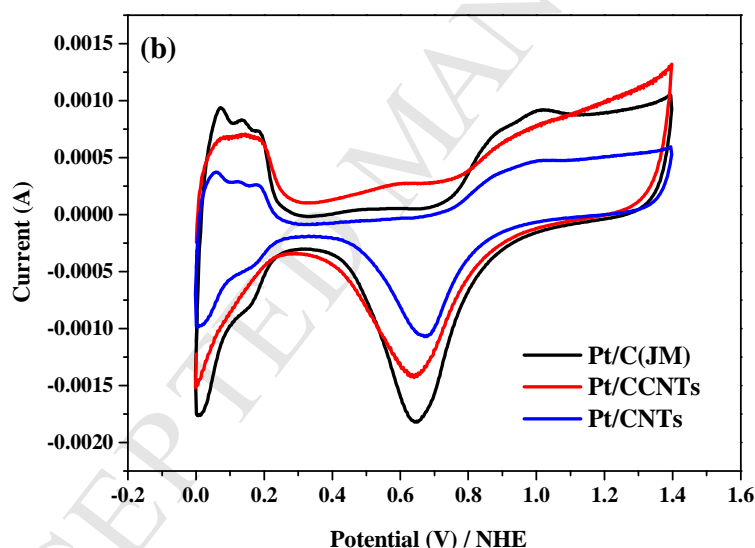
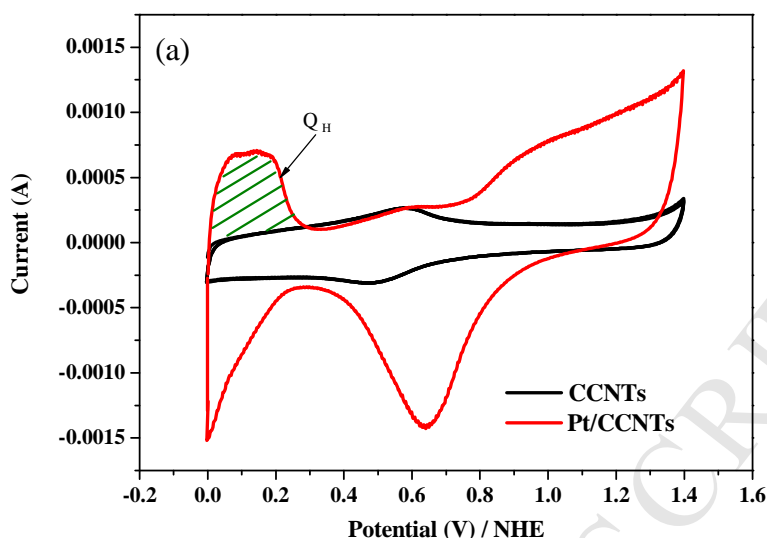
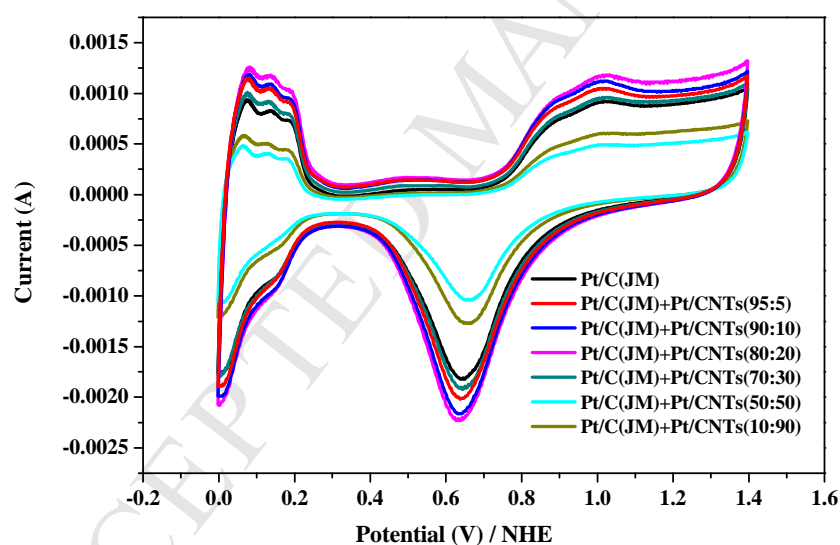


Fig. 6. Cyclic voltammograms of (a) Pt/CCNTs and CCNTs and (b) Pt/C (JM), Pt/CCNTs, and Pt/CNTs catalysts in 0.5 M H₂SO₄ with a scan rate of 20 mV s⁻¹ at room temperature.

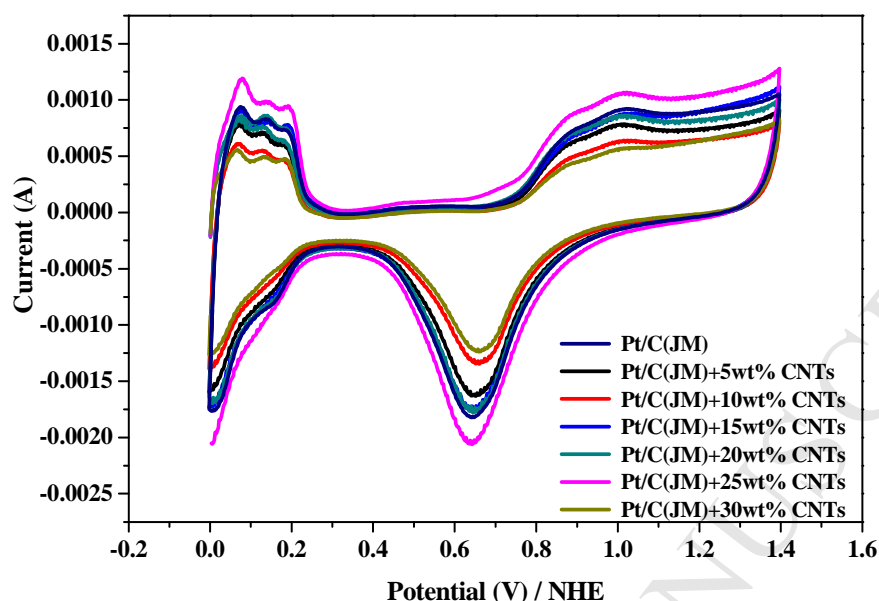
The cyclic voltammograms of Pt/CCNTs and CCNTs are shown in Fig. 6a. The ECSA of Pt can be calculated using Eq. (1) from the hydrogen electrooxidation peak after subtraction of double layer capacitance [25]. The charge of full coverage for clean polycrystalline Pt is $Q_H = 210 \mu\text{C cm}^{-2}$. L_{Pt} is the Pt loading on working electrode and A_g is the geometric surface area of the glassy carbon electrode.

$$\text{ECSA (m}^2 \text{ g}_{\text{Pt}}^{-1}) = \left[\frac{Q_{\text{H}} (\text{C})}{210 \mu\text{C cm}_{\text{Pt}}^{-2} L_{\text{Pt}} (\text{mg}_{\text{Pt}} \text{ cm}^{-2}) A_{\text{g}} (\text{cm}^2)} \right] 10^5 \quad (1)$$

Fig. 6b shows cyclic voltammograms of Pt-electrocatalysts scanned from -0 to 1.4 V vs. NHE at a scan rate of 20 mV s⁻¹ in 0.5 M H₂SO₄. According to Eq. (1), the ECSAs for Pt/C (JM), Pt/CNTs, and Pt/CCNTs are calculated to be 70, 38, and 65 m² g_{Pt}⁻¹, respectively. The result is consistent with the mean size of Pt obtained from XRD corresponding to 3.5 nm, 5.8 nm, and 3.7 nm, respectively. Although the activities for Pt/CNTs and Pt/CCNTs are inferior to commercial Pt/C, addition of Pt/CNTs and/or Pt/CCNTs into the Pt/C (JM) catalyst can improve the catalytic activity of the commercial catalyst significantly from the below results.



222 **Fig. 7.** Cyclic voltammograms of the mixed Pt/C and Pt/CNTs in 0.5M H₂SO₄ with a scan rate of
 223 20 mV s⁻¹ at room temperature.



224
 225 **Fig. 8.** Cyclic voltammograms of Pt/C with different amounts of CNTs in 0.5M H₂SO₄ with a scan
 226 rate of 20 mV s⁻¹ at room temperature.

227 ECSAs for mixed catalysts of each two kinds of Pt catalysts with different mass
 228 ratios are evaluated from CV. CV curves of the mixed Pt/C and Pt/CNTs catalysts
 229 with mass ratios of 70:30, 80:20, 90:10, and 95:5 are shown in Fig. 7, and their
 230 corresponding ECSA are 74, 90, 84, and 79 m² g_{Pt}⁻¹, respectively. The optimum ratio
 231 of Pt/C to Pt/CNTs is 80:20, its ECSA is 20 m² g_{Pt}⁻¹ higher than that of Pt/C (JM)
 232 catalyst, even the individual Pt/CNTs shows much less poor activity. It is most likely
 233 due to the fact that CNTs form a multi-dimensional network structure and establish a
 234 better conductive path [26]. However, if more than 50 wt.% of Pt/CNTs is added, a
 235 decrease in ECSA is observed. This is mainly due to the less catalytic activity
 236 contribution originated from Pt/CNTs. In order to explore the role of CNTs, CVs of
 237 Pt/C with different amounts of CNTs are shown in Fig. 8. It can be seen that Pt/C with

238 25 wt.% CNTs exhibits the highest ECSA of $135.5 \text{ m}^2 \text{ g}_{\text{Pt}}^{-1}$, which is obviously higher
239 than that of Pt/C with 5 wt.% CNTs, 10 wt.% CNTs, 15 wt.% CNTs, 20 wt.% CNTs,
240 and 30 wt.% CNTs, and their corresponding ECSAs are 77, 78, 88, 100, and $79 \text{ m}^2 \text{ g}_{\text{Pt}}^{-1}$,
241 respectively. The result indicates that adding too large or small amount of CNTs
242 induces a decrease in ECSA. With the CNTs content increasing, the ECSA increases
243 at first which can be attributed to the formation of porous network structure, but
244 decreases with the excess amount of CNTs because CNTs itself does not have
245 catalytic activity.

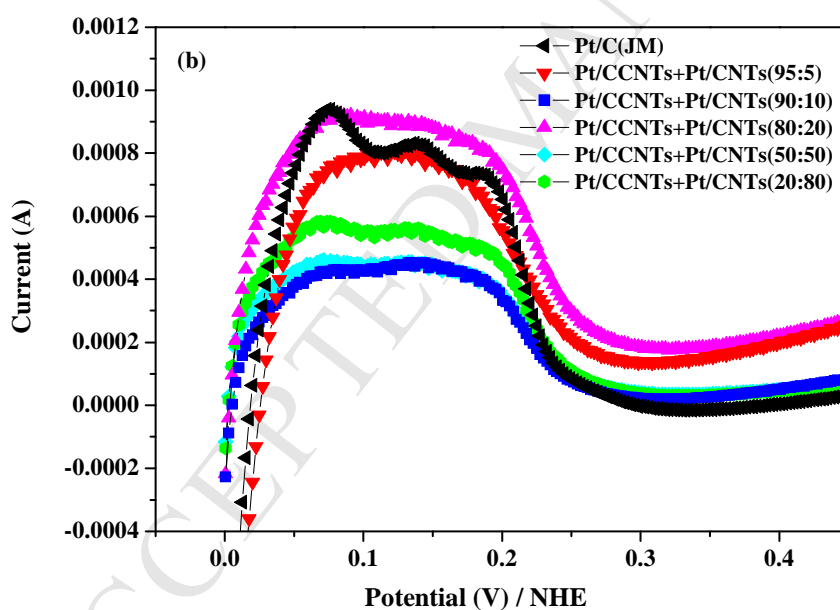
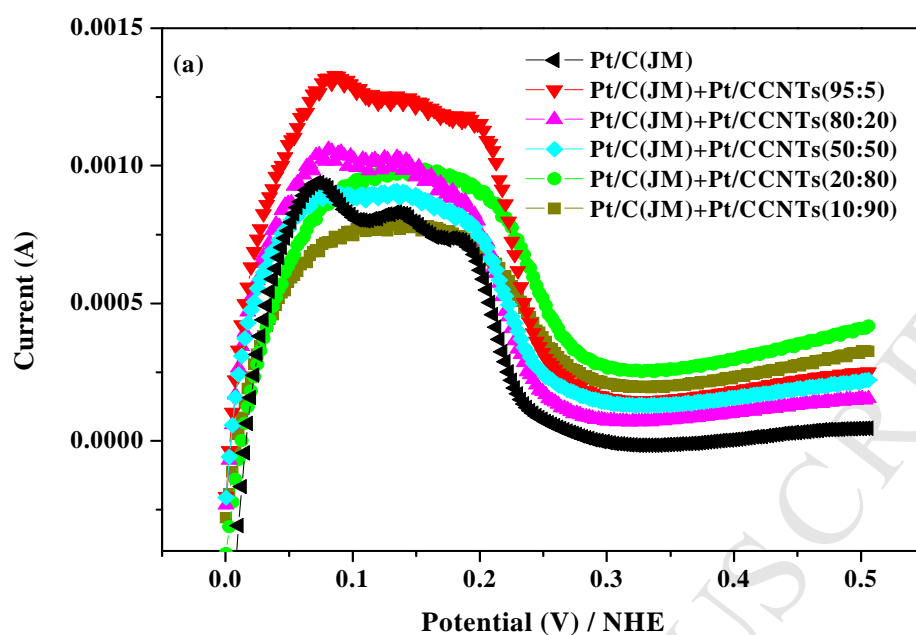
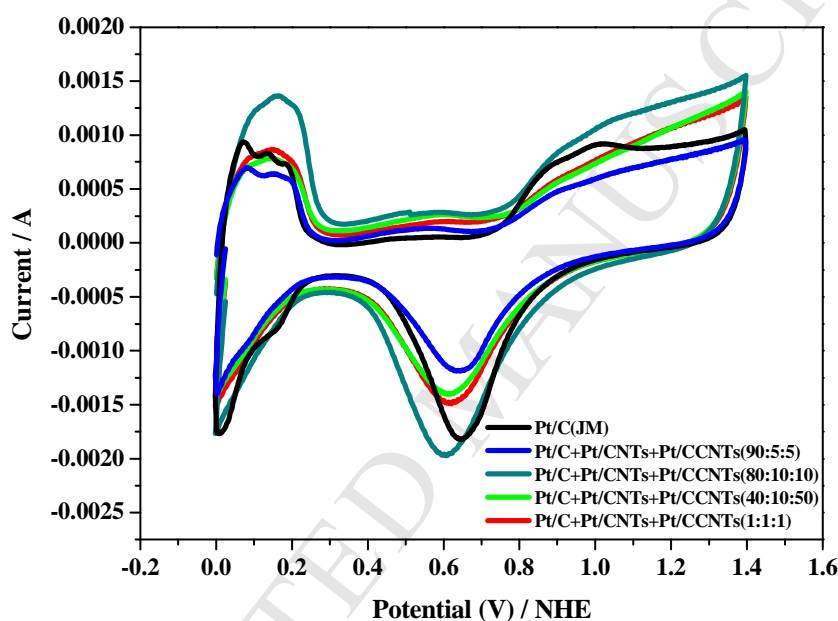


Fig. 9. Cyclic voltammograms of (a) the mixed Pt/C with Pt/CCNTs, and (b) mixed Pt/CCNTs with Pt/CNTs in 0.5M H₂SO₄ with a scan rate of 20 mV s⁻¹ at room temperature. [Only part CV curves were shown in a potential window of 0 to 0.5 V].

ECSA data calculated from Fig. 9a exhibits that the optimum ratio of Pt/C to Pt/CCNTs is 95:5 with the ECSA value of 106 m² g_{Pt}⁻¹. According to BJH result, CCNTs exhibit a uniform pore size distribution (10-40 nm) and better pore volume

254 with the increased special surface area. It proves that a very small amount of three-
 255 dimensional porous CCNTs incorporated with zero-dimensional XC-72 could
 256 contribute a higher ECSA. Meanwhile, the mixed Pt/CCNTs and Pt/CNTs catalysts
 257 with mass ratio of 80:20 as shown in Fig. 9b presents a similar ECSA value of 69 m^2
 258 $\text{g}_{\text{Pt}}^{-1}$ to that of Pt/C (JM) catalyst, even individual Pt/CCNTs or Pt/CNTs catalyst
 259 demonstrates poor catalytic activity.



260

261 **Fig. 10.** Cyclic voltammograms of the mixed Pt/C with Pt/CNTs and Pt/CCNTs in 0.5 M H_2SO_4

262 with a scan rate of 20 mV s^{-1} at room temperature.

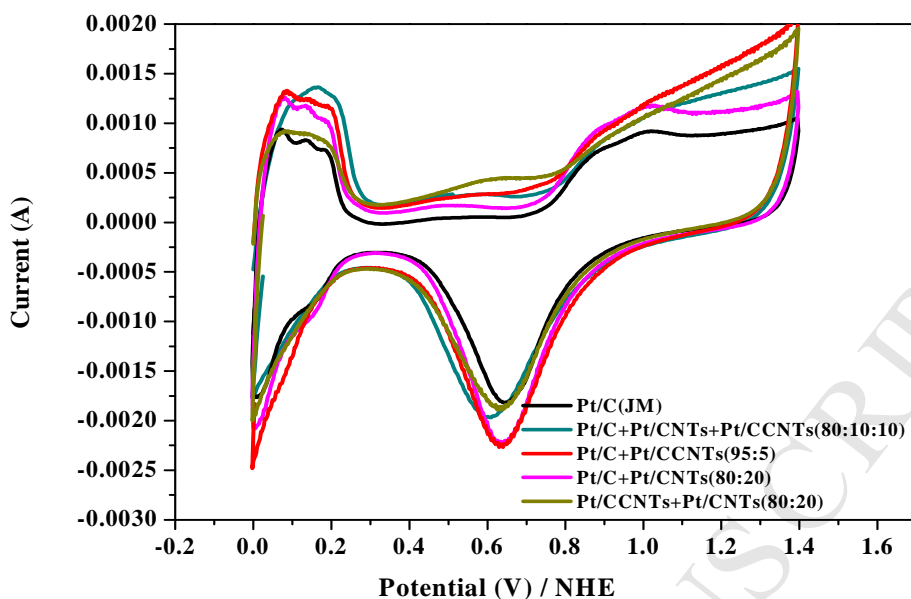


Fig. 11. Cyclic voltammograms of the optimum electrocatalysts in 0.5 M H₂SO₄ with a scan rate of 20 mV s⁻¹ at room temperature.

In Fig. 10, the mixed Pt/C, Pt/CNTs, and Pt/CCNTs with mass ratio of 80:10:10 produces the highest ECSA value of 111 m² g_{Pt}⁻¹. The three kinds of above catalysts with mass ratio of 40:10:50 or 1:1:1 exhibit the similar Pt-H oxidation region with Pt/C (JM). However, more than 80 wt.% of Pt/C leads ECSA decrease, because it needs more CNTs or CCNTs to construct multi-dimensional structure and contact well each other [27]. CVs of the optimized two and three kinds of mixed catalysts are shown in Fig. 11. The remarkable enhancing activity of Pt/C-Pt/CNTs-Pt/CCNTs can be explained in three aspects. Firstly, the multilayer compressed structure is avoided due to the addition of one-dimensional Pt/CNTs and three-dimensional Pt/CCNTs. Additionally, Pt/CCNTs-Pt/CNTs work as a multi-dimensional network, promoting electrolyte through the surface of catalysts. Ultimately, we can speculate catalytic activity contribution mainly originated from Pt/C, however, the mixed Pt/C with appropriate amount of Pt/CNTs and/or Pt/CCNTs offered much higher ECSA values.

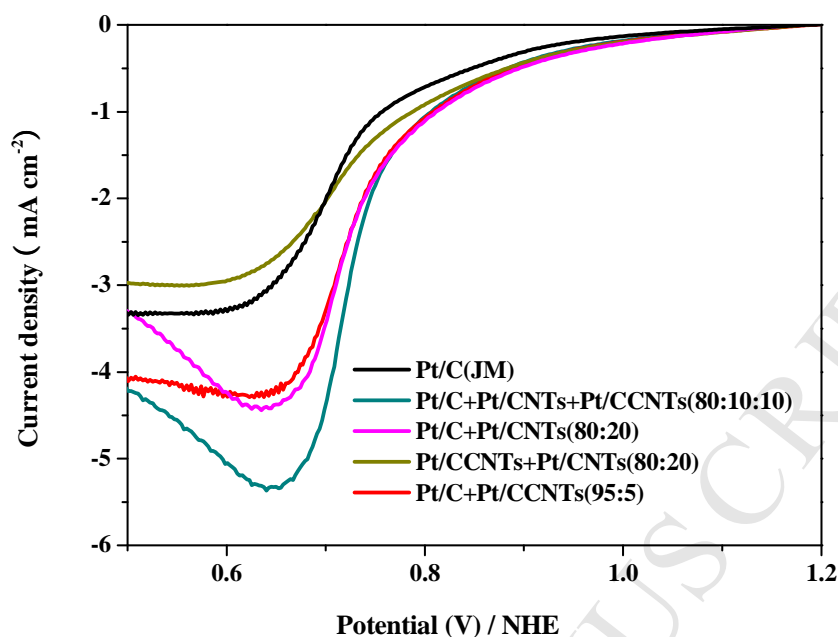


Fig. 12. LSV curves of the optimum electrocatalysts in O_2 -saturated 0.5 M H_2SO_4 with a scan rate of 20 mV s^{-1} at room temperature and a rotation rate of 1600 rpm.

LSV are taken to evaluate the ORR activity of catalysts. Fig. 12 shows LSV curves for the mixed two and three kinds of catalysts. The onset potential of mixed Pt/C-Pt/CNTs-Pt/CCNTs catalysts with mass ratio of 80:10:10 is 1.1 V and similar to the commercial Pt/C catalyst. At potential of 0.7 V (vs. NHE), the current densities of Pt/C-Pt/CNTs-Pt/CCNTs, Pt/C-Pt/CCNTs, Pt/C-Pt/CNTs, and Pt/CCNTs-Pt/CNTs are 4.7, 3.4, 3.2, and 2.2 mA cm^{-2} , compared to 2.1 mA cm^{-2} of Pt/C, indicate that the mixed two or three kinds of catalysts exhibit better ORR activity. This improvement can be attributed to the more efficient mass transport in the higher current density regions, facilitating O_2 diffusion among the catalyst layers and easily get access to Pt active sites. These results are consistent with the increased ECSAs obtained from CVs.

Electrocatalytic reaction region involves solid, liquid, and gas phase transport and electron/proton transfer [28]. Based on the morphology of three-phase region, two and

three of mixed electrocatalysts with different mass ratios are employed to construct a multi-dimensional network for the sake of optimizing electrode structure: allow reactant (O_2) more easily to get access to the active sites and the product (H_2O) to be quickly removed from them, thus assure the oxygen reduction reaction goes smoothly. The unique structure of Pt/C-Pt/CNTs-Pt/CCNTs is advantageous for ORR pathway compared to the individual Pt/CNTs, Pt/CCNTs or Pt/C. XC-72 is a good support to disperse precious metal particles, CNTs plays the role of transferring electrons, and CCNTs is responsible for constructing preferable mass transportation channels. Finally, we conceive that the mixed Pt/C with Pt/CNTs and Pt/CCNTs could be used to offer more active sites, more favorable gas-diffusion channels, and lower resistant charge-transfer paths.

4. Conclusions

In this research, each two and three kinds of Pt/C, Pt/CNTs, and Pt/CCNTs are mixed with different mass ratios. The specific active surface areas of the mixed Pt/C and Pt/CCNTs with mass ratio of 95:5 and mixed Pt/C with Pt/CNTs and Pt/CCNTs with mass ratio of 80:10:10 are calculated to be $106\text{ m}^2\text{ g}_{Pt}^{-1}$ and $111\text{ m}^2\text{ g}_{Pt}^{-1}$ with respect to $70\text{ m}^2\text{ g}_{Pt}^{-1}$ of commercial Pt/C catalyst due to the unique structure of CCNTs and the enhanced conductivity of CNTs. LSV results also confirm the improved ORR activity of the mixed Pt/C with Pt/CNTs and/or Pt/CCNTs. These results indicate that two and three of mixed platinum electrocatalysts supported on various carbon materials can significantly enhance the performance and utilization of the catalysts, and this result can be applied in practical fuel cell stacks to better the performance and reduce the amount of catalyst.

Acknowledgements

This work was supported by the Technology Project of Education Department of

Sichuan Province (13ZA0193), Innovative Research Team of Southwest Petroleum University (2012XJZT002), and Scientific Research Foundation for Returned Scholars, Ministry of Education of China.

References

- [1] E. Reddington, A. Sapienza, B. Gurau, R. Viswanathan, S. Sarangapani, E.S. Smotkin, T.E. Mallouk, *Science* 280 (1998) 1735-1737.
- [2] M. Hogarth, T. Ralph, *Platinum Met. Rev.* 46 (2002) 146-164.
- [3] T.S. Ahmadi, Z.L. Wang, T.C. Green, A. Henglein, M.A. El-Sayed, *Science* 272 (1996) 1924-1925.
- [4] M.K. Debe, *Nature* 486 (2012) 43-51.
- [5] S.H. Tang, G.Q. Sun, J. Qi, S.G. Sun, J.S. Guo, Q. Xin, G.M. Haarberg, *Chin. J. Catal.* 31 (2010) 12-17.
- [6] J.S. King, A. Wittstock, J. Biener, S.O. Kucheyev, Y.M. Wang, T.F. Baumann, S.K. Giri, A.V. Hamza, M. Baeumer, S.F. Bent, *Nano Lett.* 8 (2008) 2405-2409.
- [7] R.Z. Yang, X.P. Qiu, H.R. Zhang, J.Q. Li, W.T. Zhu, Z.X. Wang, X.J. Huang, L.Q. Chen, *Carbon* 43 (2005) 11-16.
- [8] N. Punbusayakul, S. Talapatra, L. Ci, W. Surareungchai, P.M. Ajayan, *Electrochem. Solid-State. Lett.* 10 (2007) 13-17.
- [9] C. Soldano, S. Kar, S. Talapatra, S. Nayak, P.M. Ajayan, *Nano Lett.* 8 (2008) 4498-4505.
- [10] S. Talapatra, S. Kar, S.K. Pal, R. Vajtai, L. Ci, P. Victor, M. Shaijumon, S. Kaur, O. Nalamasu, P.M. Ajayan, *Nat. Nano* 1 (2006) 112-116.
- [11] T. Hyeon, S. Han, Y. E. Sung, K. W. Park, Y. W. Kim, *Angew. Chem. Int. Ed.* 42 (2003) 4488-4492.

- 344 [12] P. Ramesh, M.E. Itkis, J.M. Tang, R.C. Haddon, J. Phys. Chem. C 112 (2008)
345 9089-9094.
- 346 [13] M.M. Shaijumon, S. Ramaprabhu, N. Rajalakshmi, Appl. Phys. Lett. 88 (2006)
347 253105-253105-3.
- 348 [14] S. Stankovich, D.A. Dikin, G.H.B. Dommett, K.M. Kohlhaas, E.J. Zimney, E.A.
349 Stach, R.D. Piner, S.T. Nguyen, R.S. Ruoff, Nature 442 (2006) 282-286.
- 350 [15] N. Behabtu, J.R. Lomeda, M.J. Green, A.L. Higginbotham, A. Sinitskii, D.V.
351 Kosynkin, D. Tsentalovich, A.N.G. Parra-Vasquez, J. Schmidt, E. Kesselman, Y.
352 Cohen, Y. Talmon, J.M. Tour, M. Pasquali, Nat. Nano 5 (2010) 406-411.
- 353 [16] S.D. Yang, C.M. Shen, X.J. Lu, H. Tong, J.J. Zhu, X.G. Zhang, H.J. Gao,
354 Electrochim. Acta 62 (2012) 242-249.
- 355 [17] R. I. Jafri, T. Arockiados, N. Rajalakshmi, S. Ramaprabhu, J. Electrochem. Soc.
356 157 (2010) 874-879.
- 357 [18] J. Qi, L.H. Jiang, S.L. Wang, G.Q. Sun, Appl. Catal. B 107 (2011) 95-103.
- 358 [19] G.S. Chai, I.S. Shin, J. S. Yu, Adv. Mater. 16 (2004) 2057-2061.
- 359 [20] N.P. Subramanian, S.P. Kumaraguru, H. Colon-Mercado, H. S. Kim, B.N. Popov,
360 T. Black, D.A. Chen, J. Power Sources 157 (2006) 56-63.
- 361 [21] M. Sevilla, C. Sanchís, T. Valdés-Solís, E. Morallón, A.B. Fuertes, J. Phys.
362 Chem. C 111 (2007) 9749-9756.
- 363 [22] K. W. Park, Y. E. Sung, S. Han, Y. Yun, T. Hyeon, J. Phys. Chem. B 108 (2004)
364 939-944.
- 365 [23] M.A. Pimenta, G. Dresselhaus, M.S. Dresselhaus, L.A. Cancodo, A. Jorio, R.
366 Sato, Phys. Chem. Chem. Phys. 9 (2007) 1276-1290.
- 367 [24] S. Mukerjee, S. Srinivasan, M.P. Soriaga, J. McRreen, J. Electrochem. Soc. 142
368 (1995) 1409-1422.

- 369 [25] Y. Garsany, O.A. Baturina, K.E. Swider-Lyons, S.S. Kocha, Anal. Chem. 82
370 (2010) 6321-6328.
- 371 [26] P. Wu, B. Li, H.D. Du, L. Gan, F.Y. Kang, Y.Q. Zeng, J. Power Sources 184
372 (2008) 381-384.
- 373 [27] C. F. Chi, M. C. Yang, H. S Weng, J. Power Sources 193 (2009) 462-469.
- 374 [28] S. Litster, G. Mclean, J. Power Sources 130 (2004) 61-76.

Highlights

CCNTs with large specific surface area and graphitic characteristic were synthesized.

Pt/C, Pt/CNTs, and Pt/CCNTs were mixed with different mass ratios and evaluated.

The ECSA of Pt/C-Pt/CNTs-Pt/CCNTs (80:10:10) were calculated to be $111 \text{ m}^2 \text{ g}_{\text{Pt}}^{-1}$.

Improved ORR activity of Pt/C-Pt/CNTs-Pt/CCNTs was obtained.